UNCLASSIFIED
SECURITY CLASSIFICATION OF THIS PAGE

MASTER COPY - FOR REPRODUCTION PURPOSES

(2)

REPORT DOCUMENTATION PAGE

1a. REPORT SECURITY CLASSIFICATION Unclassified	1b. RESTRICTIVE MARKINGS
2a. SECURITY CLASSIFICATION AUTHORITY	3. DISTRIBUTION/AVAILABILITY OF REPORT Approved for public release; distribution unlimited.
2b. DECLASSIFICATION/DOWNGRADING SCHEDULE	
4. PERFORMING ORGANIZATION REPORT NUMBER(S) AD-A209 116	5. MONITORING ORGANIZATION REPORT NUMBER(S) ARO 25575.4-EG-S
6a. NAME OF PERFORMING ORGANIZATION JAI Associates 6b. OFFICE SYMBOL (If applicable)	7a. NAME OF MONITORING ORGANIZATION U. S. Army Research Office
6c. ADDRESS (City, State, and ZIP Code) JAI Associates Mountain View, CA 94043-2216	7b. ADDRESS (City, State, and ZIP Code) P. O. Box 12211 Research Triangle Park, NC 27709-2211
8a. NAME OF FUNDING/SPONSORING ORGANIZATION U. S. Army Research Office 8b. OFFICE SYMBOL (If applicable)	9. PROCUREMENT INSTRUMENT IDENTIFICATION NUMBER DAAL03-88-C-0006
8c. ADDRESS (City, State, and ZIP Code) P. O. Box 12211 Research Triangle Park, NC 27709-2211	10. SOURCE OF FUNDING NUMBERS PROGRAM ELEMENT NO. / PROJECT NO. / TASK NO. / WORK UNIT ACCESSION NO.

11. TITLE (Include Security Classification)
Navier-Stokes Simulation of Unsteady Three-Dimensional Blade-Vortex Interactions

12. PERSONAL AUTHOR(S)
G.R. Srinivasan

13a. TYPE OF REPORT	13b. TIME COVERED	14. DATE OF REPORT (Year, Month, Day)	15. PAGE COUNT
Reprint	FROM _____ TO _____		

16. SUPPLEMENTARY NOTATION
The view, opinions and/or findings contained in this report are those of the author(s) and should not be construed as an official Department of the Army position, policy, or decision, unless so designated by other documentation.

17. COSATI CODES		
FIELD	GROUP	SUB-GROUP

18. SUBJECT TERMS (Continue on reverse if necessary and identify by block number)

19. ABSTRACT (Continue on reverse if necessary and identify by block number)

ABSTRACT ON REPRINT

20. DISTRIBUTION/AVAILABILITY OF ABSTRACT	21. ABSTRACT SECURITY CLASSIFICATION
☐ UNCLASSIFIED/UNLIMITED ☐ SAME AS RPT. ☐ DTIC USERS	Unclassified
22a. NAME OF RESPONSIBLE INDIVIDUAL	22b. TELEPHONE (Include Area Code) / 22c. OFFICE SYMBOL

DD FORM 1473, 84 MAR — 83 APR edition may be used until exhausted. All other editions are obsolete.

SECURITY CLASSIFICATION OF THIS PAGE
UNCLASSIFIED

FED-Vol. 66

ADVANCES AND APPLICATIONS IN COMPUTATIONAL FLUID DYNAMICS

presented at

THE WINTER ANNUAL MEETING OF
THE AMERICAN SOCIETY OF MECHANICAL ENGINEERS
CHICAGO, ILLINOIS
NOVEMBER 27-DECEMBER 2, 1988

sponsored by

THE FLUIDS ENGINEERING DIVISION, ASME

edited by

O. BAYSAL
OLD DOMINION UNIVERSITY

THE AMERICAN SOCIETY OF MECHANICAL ENGINEERS
United Engineering Center 345 East 47th Street New York, N.Y. 10017

NAVIER-STOKES SIMULATION OF UNSTEADY THREE-DIMENSIONAL BLADE-VORTEX INTERACTIONS

G. R. Srinivasan
JAI Associates Inc.
Mountain View, California

W. J. McCroskey
U.S. Army Aeroflightdynamics Directorate — AVSCOM
NASA Ames Research Center
Moffett Field, California

ABSTRACT

The unsteady, viscous, three-dimensional flow field of a helicopter rotor blade encountering a passing vortex is calculated by solving the thin layer Navier-Stokes equations by a finite-difference numerical procedure. A prescribed vortex method is adopted to preserve the structure of the interacting concentrated vortex. The test cases considered correspond to the experimental model rotor test conditions of Caradonna et al.[1,2]

NOMENCLATURE

a_∞	=	characteristic velocity scale, speed of sound
C	=	characteristic length scale, chord of the blade
C_p	=	pressure coefficient
e	=	total energy per unit volume
$\hat{F}, \hat{G}, \hat{H}$	=	flux vectors
M_∞	=	free-stream Mach number
M_{tip}	=	tip Mach number of the rotor blade
p	=	static pressure
Pr	=	Prandtl number
$\hat{Q}$	=	flowfield vector
r_B	=	rotor reference station
R	=	rotor radius
$R(t)$	=	rotational matrix, see Eq. (7)
Re	=	Reynolds number
$\hat{S}$	=	viscous flux vector
u_∞	=	free stream velocity
u, v, w	=	velocity components
U, V, W	=	contravariant velocity components
x, y, z, t	=	inertial coordinates
$\tilde{x}, \tilde{y}, \tilde{z}, \tilde{t}$	=	blade attached coordinates
γ	=	ratio of specific heats
Γ	=	dimensionless strength of tip vortex
θ	=	pitch angle of the rotor blade
μ	=	viscosity coefficient, advance ratio
ξ, η, ζ, τ	=	generalized curvilinear coordinates
ρ	=	density
ψ	=	azimuth angle
Ω	=	angular velocity of the rotor

INTRODUCTION

The accurate simulation of the flowfield of a helicopter rotor is still one of the most complex and challenging problems of applied aerodynamics. This is true inspite of the availability of the present day supercomputers of Cray-2 class and improved numerical algorithms. The flowfield is three-dimensional, unsteady and viscous, with pockets of transonic flow near the blade tips on the advancing side and regions of dynamic stall pockets on the retreating blades. In addition, the blades also shed complex vortical wakes; the concentrated tip vortex of each blade generally passes close to the following blades. The close encounter of these (force free) concentrated vortices with the rotor blades is often the cause of unsteady load fluctuations and acoustic noise. Figure 1 shows, through a schematic, the various complexities associated with the flowfield of a typical helicopter rotor in forward flight.

The spiralling vortex sheet emanating from each of the blades of the rotor has a profound influence on the performance of the helicopter. It not only alters the effective pitch angle of the blades and thus the airloads, but also produces highly nonlinear interactions of the vortex with the rotor flowfield. This might result many times in shock induced boundary layer separation

with associated loss of lift and increased drag. An accurate simulation of the rotor flowfield, therefore, must consider the

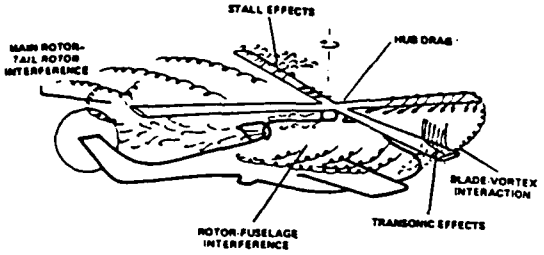

Fig. 1 Schematic of complex flowfield of a helicopter rotor

induced effects of the vortex wake including effects of blade-vortex interactions (BVI). Numerical simulation of vortex wakes is being attempted only recently after the bigger and faster computers have become available (see for example Ref. 3) and have some limited success so far. On the otherhand, much of the progress made to date in modelling the blade-vortex interaction has been hampered by the lack of the development of theoretical and/or numerical techniques to preserve the structure of the concentrated vortices in the flowfield without significant diffusion. The study of blade-vortex interaction has been the subject of numerous research papers recently.[4-9] Among these studies, some of the methods proposed[5-7] are not only very promising in preserving the concentrated vortices but have actually demonstrated to perform satisfactorily, atleast, in two-dimensional interactions. For example, Fig. 2 shows a comparison of experimental data of Caradonna et al.[1] with the unsteady, viscous,

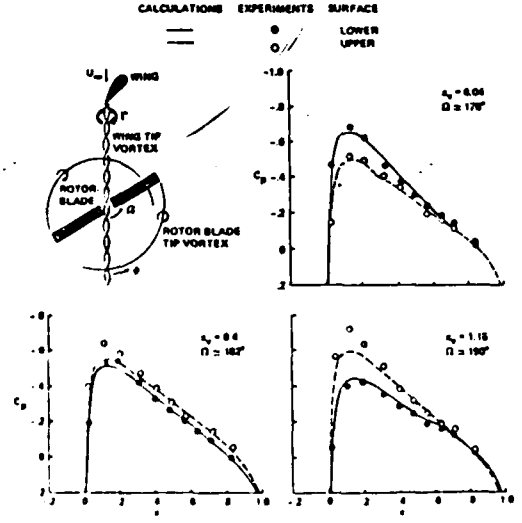

Fig. 2 Comparison of calculations and experiments for instantaneous surface pressures during a blade-vortex interaction. $M_{tip} = 0.6$, $\mu = 0.2$.

two-dimensional calculations of Srinivasan et al.[8]. This method used a prescribed vortex approach for preserving the convecting vortex.[7] Although for the subcritical flow condition of Fig. 2, the comparison of calculations with data is excellent, at the supercritical flow conditions the shock wave dominates the flowfield and the time lag effects in shock wave growth and subsequent decay become a dominant factor. In addition, three-dimensional effects get accentuated in the presence of shock waves. Hence a two-dimensional representation of such a flowfield is inadequate as observed in the study of Ref. 8.

The purpose of this paper is to calculate accurately the unsteady interaction flowfield measured in a laboratory experiment by Caradonna et al.[1,2] on a model helicopter rotor consisting of both the parallel and skewed blade-vortex interactions. In this experiment, the interacting vortex was generated upstream of the model rotor by means of a wing.

GOVERNING EQUATIONS AND NUMERICAL SCHEME

The unsteady, viscous flowfield calculations are performed using a recently developed thin layer Navier-Stokes code specifically written for helicopter rotor applications.[10] The governing partial differential equations are the unsteady, thin-layer Navier-Stokes equations. For generality, these equations are transformed from the Cartesian reference frame (x, y, z, t) to the arbitrary curvilinear space (ξ, η, ζ, τ) while retaining strong conservation law-form to capture shock waves. The transformed equations, following Ref. 7, can be written as

$$\partial_\tau(\hat{Q} - \hat{Q}_\circ) + \partial_\xi(\hat{F} - \hat{F}_\circ) + \partial_\eta(\hat{G} - \hat{G}_\circ) + \partial_\zeta(\hat{H} - \hat{H}_\circ) = Re^{-1}\partial_\zeta \hat{S} \tag{1}$$

where

$$\hat{Q} = J^{-1}\begin{bmatrix}\rho\\ \rho u\\ \rho v\\ \rho w\\ e\end{bmatrix}, \qquad \hat{F} = J^{-1}\begin{bmatrix}\rho U\\ \rho uU + \xi_x p\\ \rho vU + \xi_y p\\ \rho wU + \xi_z p\\ U(e+p) - \xi_t p\end{bmatrix}$$

$$\hat{G} = J^{-1}\begin{bmatrix}\rho V\\ \rho uV + \eta_x p\\ \rho vV + \eta_y p\\ \rho wV + \eta_z p\\ V(e+p) - \eta_t p\end{bmatrix}, \hat{H} = J^{-1}\begin{bmatrix}\rho W\\ \rho uW + \zeta_x p\\ \rho vW + \zeta_y p\\ \rho wW + \zeta_z p\\ W(e+p) - \zeta_t p\end{bmatrix}$$

Here $\hat{Q}$ is the flowfield vector we are solving for and $\hat{Q}_\circ$ is the solution of the Euler equations for a line vortex convecting in a uniform free stream. $\hat{F}$, $\hat{G}$, $\hat{H}$ and $\hat{F}_\circ$, $\hat{G}_\circ$, $\hat{H}_\circ$ are the appropriate flux vectors for the two flows. The contravariant velocity

components U, V and W are defined as

$$U = \xi_t + \xi_x u + \xi_y v + \xi_z w$$
$$V = \eta_t + \eta_x u + \eta_y v + \eta_z w$$
$$W = \zeta_t + \zeta_x u + \zeta_y v + \zeta_z w$$

The viscous flux vector $\hat{S}$, written here in the limit of thin-layer approximation, is given by

$$\hat{S} = J^{-1} \begin{bmatrix} 0 \\ \mu m_1 u_\zeta + (\mu/3) m_2 \zeta_x \\ \mu m_1 v_\zeta + (\mu/3) m_2 \zeta_y \\ \mu m_1 w_\zeta + (\mu/3) m_2 \zeta_z \\ \mu m_1 m_3 + (\mu/3) m_2 (\zeta_x u + \zeta_y v + \zeta_z w) \end{bmatrix}$$

where

$$m_1 = \zeta_x^2 + \zeta_y^2 + \zeta_z^2$$
$$m_2 = \zeta_x u_\zeta + \zeta_y v_\zeta + \zeta_z w_\zeta$$
$$m_3 = \frac{1}{2}(u^2 + v^2 + w^2)_\zeta + \kappa Pr^{-1}(\gamma - 1)^{-1}(a^2)_\zeta$$

In this equation, κ is the coefficient of thermal conductivity, Re is the Reynolds number, Pr is the Prandtl number, a is the speed of sound and J is the transformation Jacobian, whose inverse is

$$J^{-1} = x_\xi y_\eta z_\zeta + x_\zeta y_\xi z_\eta + x_\eta y_\zeta z_\xi - x_\xi y_\zeta z_\eta - x_\eta y_\xi z_\zeta - x_\zeta y_\eta z_\xi$$

The primitive variables of Eq. (1), viz., the density ρ, the mass fluxes $\rho u, \rho v, \rho w$ and the energy per unit volume e, are normalized by the free stream reference quantities. The reference length scale is C and the reference time scale is C/a_∞. The details on the metrics of the transformation $(\xi_t, \xi_x, \xi_y, \xi_z)$, $(\eta_t, \eta_x, \eta_y, \eta_z)$ and $(\zeta_t, \zeta_x, \zeta_y, \zeta_z)$ can be found in Ref. 11.

The velocity components u, v, w and the pressure, p, are related to the total energy per unit volume, e, through the equation of state for a perfect gas by

$$p = (\gamma - 1)(e - \frac{\rho}{2}(u^2 + v^2 + w^2)) \tag{2}$$

where γ is the ratio of specific heats.

In the above equations u, v, and w are the Cartesian components of the velocity in the inertial coordinate system (x, y, z, t). In the present formulation Eq. (1) is solved in the inertial frame of reference. The inertial coordinates $\mathbf{X} = (x, y, z, t)$ are related to the blade fixed coordinates $\mathbf{X_b} = (\bar{x}, \bar{y}, \bar{z}, \bar{t})$ through the relation given by

$$\begin{aligned} \mathbf{X}(x, y, z) &= \mathbf{R}(t)\mathbf{X_b}(\bar{x}, \bar{y}, \bar{z}) \\ t &= \bar{t} \end{aligned} \tag{3}$$

where $\mathbf{R(t)}$ is the rotational matrix[12] given by

$$R(t) = \begin{bmatrix} \cos\Omega\bar{t} & -\sin\Omega\bar{t} & 0 \\ \sin\Omega\bar{t} & \cos\Omega\bar{t} & 0 \\ 0 & 0 & 1 \end{bmatrix} \tag{4}$$

Here Ω is the rotational frequency of the rotor and Ωt represents the azimuth sweep of the rotor blade.

The equation set, Eq. (1), is solved using an implicit, approximately-factored numerical scheme, developed by Ying et al.,[13] that uses spatial central-differencing in the η and ζ directions and upwind-differencing in the ξ direction. The flux vector $\hat{F}$ has been split into $\hat{F}^+$ and $\hat{F}^-$ according to its eigenvalues and the algorithm is given by

$$\begin{aligned} &\left[I + h\delta_\xi^b(\hat{A}^+)^n + h\delta_\zeta \hat{C}^n - hRe^{-1}\bar{\delta}_\zeta J^{-1}\hat{M}^n J - D_i|_\zeta\right] \\ &\times \left[I + h\delta_\xi^f(\hat{A}^-)^n + h\delta_\eta \hat{B}^n - D_i|_\eta\right](\Delta\hat{Q}^n - \Delta\hat{Q}_\circ^n) = \\ &- \Delta t\{\delta_\xi^b[(\hat{F}^+)^n - \hat{F}_\circ^+] + \delta_\xi^f[(\hat{F}^-)^n - \hat{F}_\circ^-] \\ &+ \delta_\eta(\hat{G}^n - \hat{G}_\circ) + \delta_\zeta(\hat{H}^n - \hat{H}_\circ) - Re^{-1}\bar{\delta}_\zeta(\hat{S}_\zeta^n)\} \\ &- (D_e|_\eta + D_e|_\zeta)(\hat{Q}^n - \hat{Q}_\circ^n) \end{aligned} \tag{5}$$

The factored operators are solved by sweeping in the ξ direction and inverting tridiagonal matrices with 5 x 5 blocks for the other two directions. Currently, a significant part of the computational time is taken to form the plus and minus Jacobian matrices for the flux vector $\hat{F}$ with this numerical scheme. Artificial dissipation terms (second- and fourth-order) have been added in the central differencing directions for stability reasons.[11] The numerical code is vectorized for the Cray-2 supercomputer.

A body conforming finite-difference grid has been used for the rectangular blade having an aspect ratio of 7 and consists of warped spherical O-O grid topology. The flowfield grid is numerically generated using the three-dimensional hyperbolic grid solver of Steger and Chaussee[14] with proper clustering in the leading and trailing edge regions and in the tip region. The grid is nearly orthogonal at the surface and the spacing in the normal direction at the surface is chosen to be 0.00006C. Although most of the computations were done with a grid topology having 155 points in the periodic direction around the airfoil, and 66 points each in the spanwise and normal directions, for a total of about 700,000 grid points, some calculations were also done on a smaller grid 34 x 99 x 31 . The outer grid boundary is chosen to be at 10 chords in all directions for both sizes.

The boundary conditions consist of surface boundary conditions and farfield boundary conditions and are applied explicitly. At the rotating blade surface because of the noslip condition, the contravariant velocities U, V and W are set to zero. However, the time metrics ξ_t, η_t and ζ_t are nonzero as the blade (and the grid attached to it) is moving in azimuth. The density at the wall is determined by assuming an adiabatic wall condition. The pressure along the body surface is calculated from the normal momentum relation (see for example Ref. 11). Having calculated the density and pressure, the total energy is determined from the equation of state.

At the farfield boundary the flow quantities are either fixed or extrapolated from the interior depending on whether the flow is subsonic or supersonic and if it is of inflow- or outflow-type at the boundary. The characteristic velocities of the Euler equations determine the number of flow properties to be specified to control the reflections of waves from the boundaries. For the subsonic-inflow boundary, four quantities must be specified. Thus, density is extrapolated while the velocities and the total energy are specified by the free stream values. For the supersonic-inflow, all flow quantities are specified. At the subsonic-outflow boundaries, only one quantity is specified, viz., pressure is fixed. For the supersonic-outflow condition all flow quantities are extrapolated from the interior. At the plane containing the blade root the condition $\partial Q/\partial y = 0$ is imposed. The interacting vortex is assumed to have an analytical representation and is initialized as described in Ref. 7. The induced velocity due to this line vortex is calculated using Biot-Savart's Law.

RESULTS

The numerical code modified for the purpose of calculating the blade-vortex interaction has been validated against experimental data of Caradonna and Tung[15] for nonlifting and lifting hover conditions at both subcritical and supercritical tip speeds in Ref. 10. The boundary layer is assumed to be turbulent in all cases considered here and an algebraic eddy viscosity model[16] is used for calculating the turbulent viscosity. Figure 3 shows a typical result for a lifting hovering rotor from Ref. 10; the comparison of the calculations with the experimental data is very good.

Before considering the interaction of the rotor flowfield with a line vortex convecting with the free stream, the flowfield of a rotor in forward flight has to be computed. As noted before[8], at the subcritical flow conditions corresponding to a $M_{tip} = 0.6$, the time lag effects and the three-dimensional effects appear negligible as shown in Fig. 4 and this is the reason that two- dimensional calculations gave excellent agreement with experiments of Caradonna et al.[1] not only for the basic rotor flow in the absence of vortex interaction, as seen in Fig. 4, but also for the blade-vortex interaction flowfield as shown in Fig. 2. It should be noted that the experiments of parallel blade-vortex

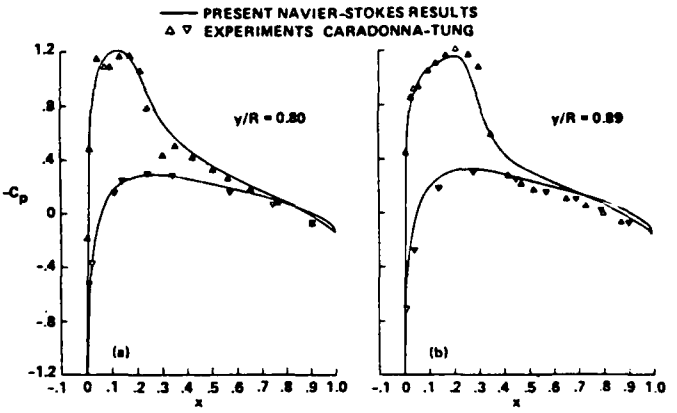

Fig. 3 Surface pressures of a lifting rotor in hover. $M_{tip} = 0.877$, $\theta = 8.0$, Re = 3.96 x 10^6.

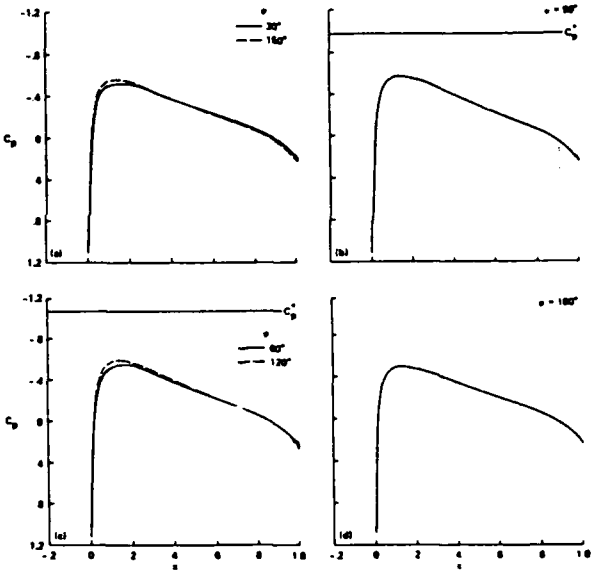

Fig. 4 Instantaneous surface pressures for a two-bladed rotor. $M_{tip} = 0.6$, $\mu = 0.2$.

interaction of Caradonna et al. were presented as test case results for validating the two-dimensional numerical calculation procedures. Although this data would provide a data source for validating the two-dimensional codes at the subcritical flow conditions, this may not be true for supercritical flow conditions as demonstrated by Srinivasan et al.[3]

At the supercritical tip flow conditions corresponding to $M_{tip} = 0.8$ with an advance ratio of 0.2, the basic rotor flowfield is dominated by the shock wave and earlier two-dimensional calculations showed strong flow three-dimensionality and un-

steady time-lags in shock formation and decay. Therefore, two-dimensional calculations failed to calculate accurately even the basic rotor flow. As shown in Figs. 5-6, the agreement of two-dimensional calculations with those of three-dimensional calculations and of experiment appears excellent in only the first quadrant of the rotor azimuth. In the begining of the second quadrant, the shock wave gets very strong as the relative blade speed reaches Mach one. For this flow, the two-dimensional assumption appears inadequate. The strengthening of the shock wave and the eventual progressive demise have strong time-lags built in to it. The flow three-dimensionality appears to be accentuated in the presence of the shock wave. Because of these features, the two-dimensional results greatly overpredict the strength of the shock wave even for the basic rotor flow (in the absence of a vortex interaction). Of course, with a vortex interaction the flowfield gets further complicated. These and other important results will be presented in the final version of the paper.

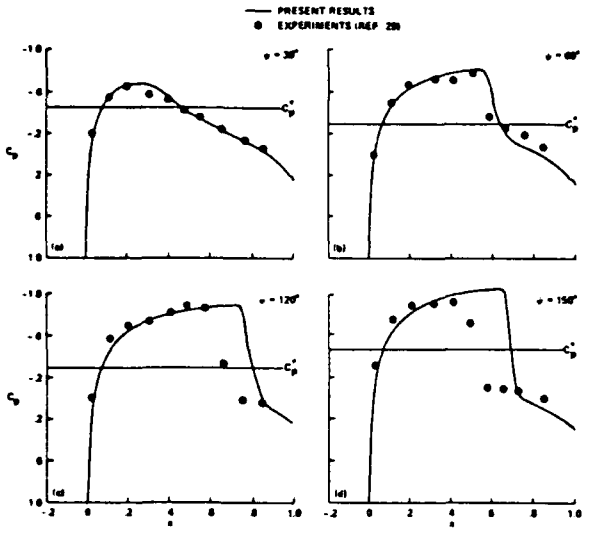

Fig. 5 Two-dimensional calculations of basic rotor flow compared with three-dimensional experimental data. $M_{tip} = 0.8$, $\mu = 0.2$.

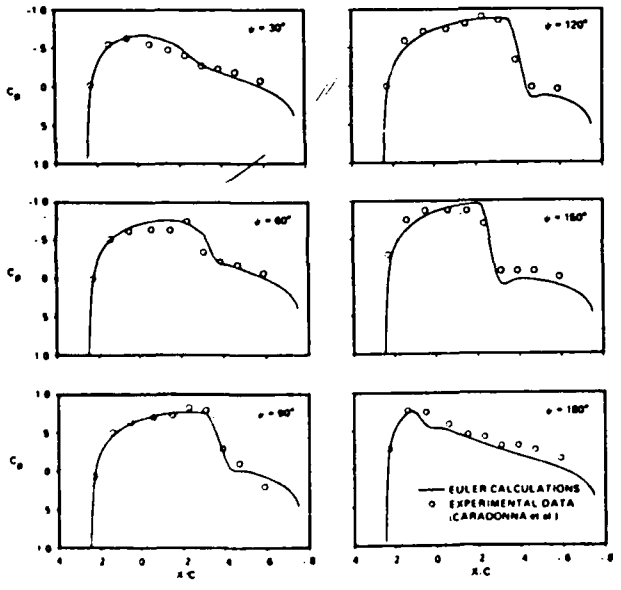

Fig. 6 Three-dimensional Euler calculations (Ref. 17) Compared with experiments (Ref. 1). $M_{tip} = 0.8$, $\mu = 0.2$.

CONCLUSIONS

A numerical procedure is presented to calculate the unsteady, viscous, three-dimensional flowfields of a helicopter rotor in forward flight and blade-vortex interactions in subcritical and supercritical flow conditions. Important flow features such as time lag effects in shock growth and demise, as well as the importance of three-dimensional effects are discussed. The test cases considered here for computations correspond to the two sets of test data generated by Caradonna et al.[1,2] on a model two-bladed rotor in a wind tunnel.

ACKNOWLEDGMENTS

The first author (GRS) would like to acknowledge the support of this research by the U. S. Army Research Office under Contract DAAL03-88-C-0006. Computational time was provided by the Applied Computational Fluids Branch of NASA Ames Research Center.

REFERENCES

1. Caradonna, F. X., Laub, G. H. and Tung, C., "An Experimental Investigation of the Parallel Blade-Vortex Interaction", Paper presented at the 10th European Rotorcraft Forum, The Hague, Netherlands, August 1984.

2. Caradonna, F. X., Lautenschlager, J. and Silva, M., "An Experimental Study of Rotor Blade-Vortex Interactions", AIAA Paper 88-0045, January 1988.

3. Srinivasan, McCroskey, W. J., Baeder, J. D., and Edwards, T. A., "Numerical Simulation of Tip Vortices of Wings in Subsonic and Transonic Flows", AIAA Paper 86-1095, May 1986; also to appear in AIAA Journal, April 1988.

4. Workshop on Blade-Vortex Interactions (unpublished), NASA Ames Research Center, Moffett Field, California, October 1984.

5. Steinhoff, J. and Suryanarayanan, K., "The Treatment of Vortex Sheets in Compressible Potential Flow", AIAA Paper 83-1881-CP, 1983.

6. Rai, M. M., "Navier-Stokes Simulation of Blade-Vortex Interaction Using High-Order Accurate Upwind Schemes", AIAA Paper 87-0543, 1987.

7. Srinivasan, G. R. and McCroskey, W. J., "Numerical Simulations of Unsteady Airfoil-Vortex Interactions", VERTICA, Vol. 11, 1987, pp. 3-28.

8. Srinivasan, G. R., McCroskey, W. J., and Baeder, J. D., "Aerodynamics of Two-Dimensional Blade-Vortex Interaction", AIAA Journal, Vol. 24, No. 10, October 1986, pp. 1569-1576.

9. Strawn, R. C. and Tung, C., "The Prediction of Transonic Loading on Advancing Helicopter Rotors", NASA TM-88238, April 1986.

10. Srinivasan, G. R. and McCroskey, W. J., "Navier-Stokes Calculations of Hovering Rotor Flowfields", AIAA Paper 87-2629-CP, August 1987; also to appear in Journal of Aircraft, July 1988.

11. Pulliam, T. H. and Steger, J. L., "Implicit Finite-Difference Simulations of Three-Dimensional Compressible Flow", AIAA Journal, Vol. 18, No. 2, February 1980, pp. 159-167.

12. Isom, M. P., "Unsteady Subsonic and Transonic Potential Flow Over Helicopter Rotor Blades", NASA CR-2463, October 1974.

13. Ying, S. X., Steger, J. L., Schiff, L. B. and Baganoff, D., "Numerical Simulation of Unsteady, Viscous, High-Angle-Of-Attack Flows Using a Partially Flux-Split Algorithm", AIAA Paper 86-2179, August 1986.

14. Steger, J. L. and Chaussee, D. S., "Generation of Body-Fitted Coordinates Using Hyperbolic Partial Differential Equations", SIAM J. Sci. Stat. Comput., Vol. 1, No. 4, December, pp. 431-437.

15. Caradonna, F. X. and Tung, C., "Experimental and Analytical Studies of a Model Rotor in Hover", VERTICA, Vol. 5, No. 2, 1981, pp. 149-161.

16. Baldwin, B. S. and Lomax, H., "Thin Layer Approximation and Algebraic Model for Separated Turbulent Flow", AIAA Paper 78-257, January 1978.

17. Chen, C. L. and McCroskey, W. J., "Numerical Simulation of Helicopter Multi-Bladed Rotor Flow", AIAA Paper 88-0046, January 1988.

UNCLASSIFIED
SECURITY CLASSIFICATION OF THIS PAGE

FOR REPRODUCTION PURPOSES

REPORT DOCUMENTATION PAGE

1a. REPORT SECURITY CLASSIFICATION Unclassified	1b. RESTRICTIVE MARKINGS
2a. SECURITY CLASSIFICATION AUTHORITY	3. DISTRIBUTION / AVAILABILITY OF REPORT Approved for public release; distribution unlimited.
2b. DECLASSIFICATION / DOWNGRADING SCHEDULE	
4. PERFORMING ORGANIZATION REPORT NUMBER(S)	5. MONITORING ORGANIZATION REPORT NUMBER(S)
6a. NAME OF PERFORMING ORGANIZATION JAI Associates, Inc 6b. OFFICE SYMBOL (If applicable)	7a. NAME OF MONITORING ORGANIZATION U. S. Army Research Office
6c. ADDRESS (City, State, and ZIP Code) P. O. Box 293, Mountain View, CA 94042	7b. ADDRESS (City, State, and ZIP Code) P. O. Box 12211 Research Triangle Park, NC 27709-2211
8a. NAME OF FUNDING / SPONSORING ORGANIZATION U. S. Army Research Office 8b. OFFICE SYMBOL (If applicable)	9. PROCUREMENT INSTRUMENT IDENTIFICATION NUMBER
8c. ADDRESS (City, State, and ZIP Code) P. O. Box 12211 Research Triangle Park, NC 27709-2211	10. SOURCE OF FUNDING NUMBERS PROGRAM ELEMENT NO. / PROJECT NO. / TASK NO. / WORK UNIT ACCESSION NO.

11. TITLE (Include Security Classification)
Navier-Stokes Simulation of Unsteady Three-Dimensional Blade-Vortex Interactions

12. PERSONAL AUTHOR(S)
G. R. Srinivasan and W. J. McCroskey

13a. TYPE OF REPORT	13b. TIME COVERED	14. DATE OF REPORT (Year, Month, Day)	15. PAGE COUNT
Reprint	FROM _____ TO _____		

16. SUPPLEMENTARY NOTATION
The view, opinions and/or findings contained in this report are those of the author(s) and should not be construed as an official Department of the Army position, policy, or decision, unless so designated by other documentation.

17. COSATI CODES			18. SUBJECT TERMS (Continue on reverse if necessary and identify by block number)
FIELD	GROUP	SUB-GROUP	Unsteady, thin layer Navier-stokes, Blade-Vortex interaction ParallelBVI, Rotor in forward flight

19. ABSTRACT (Continue on reverse if necessary and identify by block number)

The viscous, unsteady, three-dimensional flow field of blade-vortex interaction is calculated by solving numerically the thin layer Navier-Stokes equations. A prescribed vortex method is adopted to preserve the structure of the interacting vortex. The test cases considered correspond to the experimental model rotor test conditions of Caradonna and Tung.

20 DISTRIBUTION / AVAILABILITY OF ABSTRACT ☐ UNCLASSIFIED/UNLIMITED ☐ SAME AS RPT. ☐ DTIC USERS	21. ABSTRACT SECURITY CLASSIFICATION Unclassified
22a NAME OF RESPONSIBLE INDIVIDUAL	22b. TELEPHONE (Include Area Code) / 22c. OFFICE SYMBOL

DD FORM 1473, 84 MAR

83 APR edition may be used until exhausted.
All other editions are obsolete.

SECURITY CLASSIFICATION OF THIS PAGE
UNCLASSIFIED